ISBN: 978-3-95450-231-8 ISSN: 2673-5490 doi: 10.18429/JACoW-IPAC2023-WEPL184

ANALYSIS OF SINGLE-BUNCH INSTABILITIES FOR DIAMOND-II

Dmitrii Rabusov*, Richard Fielder, Siwei Wang, Diamond Light Source, Oxfordshire, UK

Abstract

Single-bunch instabilities are among the major effects limiting beam intensity in synchrotrons. In the case of a light source with ultra-low emittances, this might be a critical issue causing poor performance of the synchrotron. This study elaborates on the case of the Diamond-II storage ring showing the results of particle simulations which include the value of the threshold current for different configurations of the latest versions of the lattice and the updated impedance model. The resulting impedance-induced betatron tune shifts, bunch lengthening, and synchrotron phase shifts obtained in simulations agree with analytical predictions. We obtain optimal parameters for horizontal and vertical chromaticities for all possible lattice and impedance configurations considering chromaticity variation as a measure to mitigate single-bunch instabilities.

INTRODUCTION

Diamond-II, the upgrade of the Diamond Light Source, is a 4th generation synchrotron radiation source. As compared with the operating machine, the vacuum vessels of Diamond-II are significantly narrower [1]. Therefore, the strength of the wake-fields increases [2], arising from the interaction between the beam and the vacuum chamber. Recent publications [3, 4] show that, for a 4th generation light source to meet its design parameters, collective effects should be accurately assessed.

UPDATE OF IMPEDANCE DATABASE

Diamond-II has a 6-fold symmetry, and there are three types of straights in a super-period (the update of the Diamond-II lattice is presented in Ref. [5]), namely 2.9 m Mid Straight, 5.1 m Standard Straight, and 7.5 m Long Straight. A single girder supports the magnets in each half of a cell. In total, there are four types of girders, Long-to-Mid (LM), Mid-to-Standard (MS), Standard-to-Mid (SM), and Mid-to-Long (ML). Previously, the impedance database and apertures (demonstrated in Refs. [1, 2]) were based on only a preliminary LM girder model. This work presents simulation results with the updated impedance database which contains revised models for LM, ML, and MS girders. Although the SM girder is not complete, it is mostly similar to the LM. Additionally, dipole vessels on all girders are assumed to have a new NEG-coated copper design rather than the previous aluminium with ante-chamber.

The geometric component of the Diamond-II impedance is calculated using CST [6]. Previously, we used a 3 mm bunch length in the CST simulations, whereas now it corresponds to 0.5 mm for most elements. Furthermore, the updated database provides output as geometric wake-functions with a length of 300 mm.

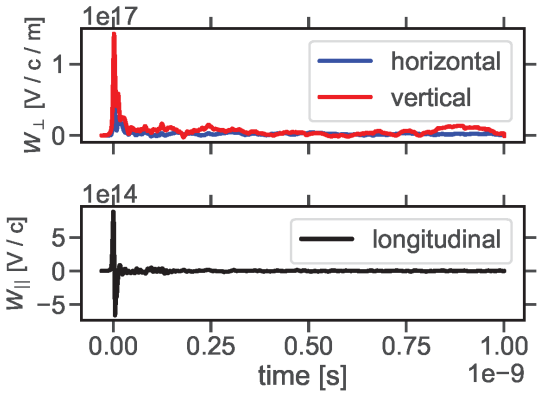

Figure 1: Geometric component of the Diamond-II wake-function when IDs are closed.

An example of the CST simulations is presented in Fig. 1, corresponding to the total geometric wake normalised with the beta-functions. In this case, all insertion devices (IDs) are closed. Blue and red lines (top) represent the transverse component while the black line (bottom) is the longitudinal one. Next, Fig. 2 shows the results of the summed resistive-wall impedance calculated using the ImpedanceWake2D [7] code.

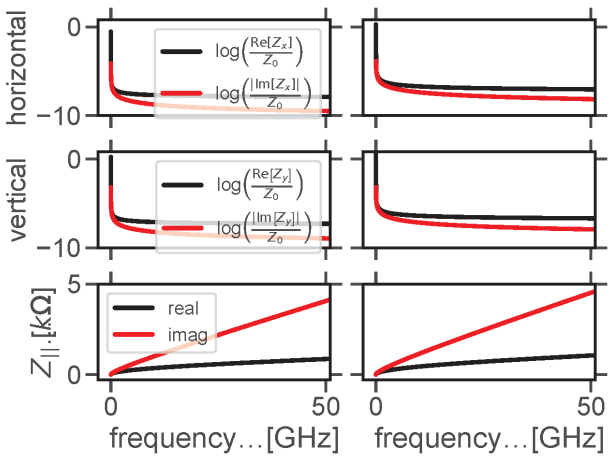

Figure 2: Resistive-wall component of the Diamond-II impedance, IDs are open (left), IDs are closed (right), reference impedance $Z_0 = 1$ GΩ.

Both real (black) and imaginary (red) components are stronger in the case when all IDs are closed (right). The span of frequencies is 81.92 GHz with a sampling step of 10 MHz in the transverse, whereas in the longitudinal, the span is 51.2 GHz with a sampling step of 100 MHz.

* dmitrii.rabusov@diamond.ac.uk

ISBN: 978-3-95450-231-8 ISSN: 2673-5490 doi: 10.18429/JACoW-IPAC2023-WEPL184

Having discussed how to construct the impedance database, the next section of this work addresses the implementation of the database's output, namely, geometric wake and the resistive-wall impedance in Elegant [8] particle simulations.

SINGLE-BUNCH EFFECTS

This work presents the results obtained with a simulation model which contains one-turn-map tracking (for single-particle effects), wake-field elements *wake* and *trwake* (for the geometric components), impedance elements *zlongit* and *ztransverse* (for the resistive-wall components), the RF cavity, the harmonic cavity (optional), and synchrotron radiation. In this study, the beam contains only a single bunch. The bunch distribution is represented by $2 \cdot 10^5$ macro particles. Diamond-II can have various filling patterns resulting in $I = 0.33$ mA per bunch nominal currents for the standard filling pattern and $I = 1.6$ mA maximum bunch current in a hybrid filling pattern.

Longitudinal

To separate longitudinal and transverse collective effects, we start with *wake* and *zlongit* wake-field elements only.

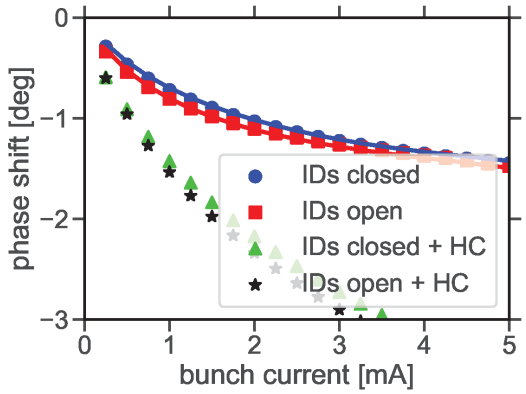

Figure 3: Synchronous phase shift with increasing bunch current, tracking results and formula.

Here and all figures below, the blue dots, red squares, green triangles, and black stars represent simulation results for closed IDs, open IDs, closed IDs with the harmonic cavity, and open IDs with the harmonic cavity respectively. The tracking results match well with the theoretically predicted phase shift (solid blue and red lines),

$$\Delta\phi_s = \frac{I \oint Z_{\parallel}(\omega)\, h(\omega)\, \mathrm{d}\omega}{2\pi f_0\, V_{\mathrm{RF}}\, \cos\phi_s}\,, \qquad (1)$$

where I is the bunch current, $Z_{\parallel}$ is the longitudinal impedance, $\omega = 2\pi f$, $h(\omega)$ is the bunch power spectrum (the bunch length is obtained from tracking to reconstruct this function), f_0 is the revolution frequency, and V_{RF} is the RF voltage.

Next, the bunch lengthening in Diamond-II is calculated analytically (using Eq. (2) which is Zotter's formula [3]) and observed in simulations, results are demonstrated in Fig. 4 as solid blue and red lines for closed and open IDs respectively.

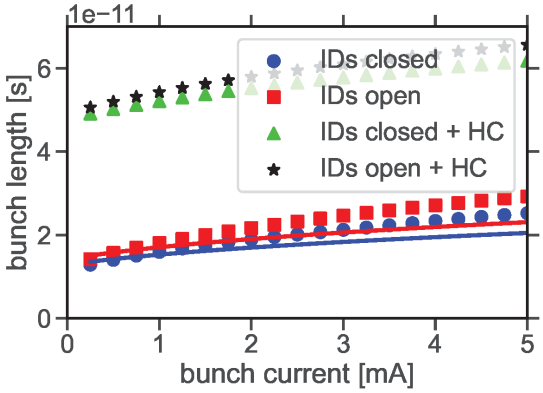

Figure 4: Current-dependent bunch lengthening.

Similarly to the results with the previous impedance model [2], the bunch length increases non-linearly with the bunch current, which can be compared to the numerical solution of

$$\left(\frac{\sigma_t}{\sigma_{t0}}\right)^3 - \frac{\sigma_t}{\sigma_{t0}} = \frac{I\,\alpha_c \oint h(\omega)\,\mathrm{Im}\left(Z_{\parallel}\right)\frac{\omega_0}{\omega}\,\mathrm{d}\omega}{4\sqrt{\pi}\,\nu_s^2\,\omega_0^3\,\sigma_{t0}^3\,E\oint h(\omega)\,\mathrm{d}\omega}\,, \qquad (2)$$

where σ_t is the bunch length, α_c is the compaction factor, ν_s is the synchrotron tune, and E is the energy in eV. A discrepancy between Eq.(2) and simulation results appears at $I > 1.5$ mA, where the bunch profile starts to deviate from a Gaussian distribution due to the microwave instability shown in Fig. 5.

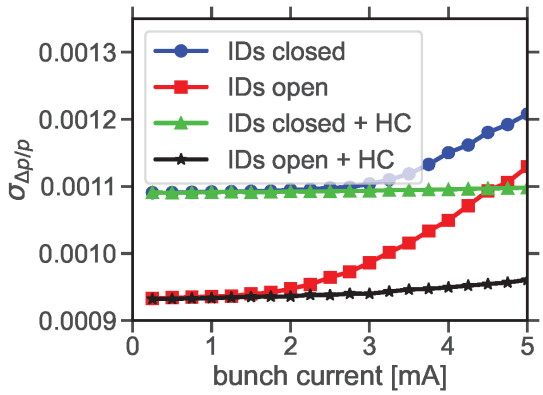

Figure 5: Momentum spread with increasing bunch current.

In the case of open and closed IDs without the harmonic cavity, the momentum spread starts increasing when the bunch current is above the microwave-instability threshold. The harmonic cavity lengthens the bunch, thereby helping to mitigate the microwave instability.

ISBN: 978-3-95450-231-8 ISSN: 2673-5490 doi: 10.18429/JACoW-IPAC2023-WEPL184

Transverse

Now, we can turn to the collective effects which appear in the horizontal and vertical planes by adding *trwake* and *ztransverse* wake-field elements into the model (longitudinal effects are also included).

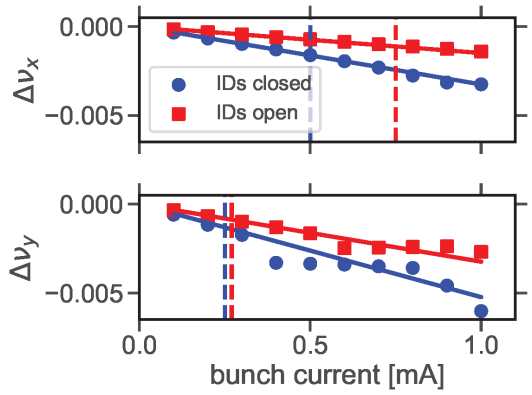

Figure 6: Current-dependent horizontal (top) and vertical (bottom) betatron tune shifts.

Figure 6 shows the tune shifts with increasing bunch current at zero chromaticity ($\xi_x = \xi_y = 0$). Simulation results agree with the analytical shift of betatron tunes (blue and red solid lines for closed and open IDs respectively) given by

$$\frac{\mathrm{d}\nu_{x,y}}{\mathrm{d}I} = -\frac{\langle \beta(s) \oint h(\omega)\,\mathrm{Im}\left(Z_{x,y}\right)\mathrm{d}\omega\rangle_s}{4\pi\,\sigma_t E \oint h(\omega)\,\mathrm{d}\omega}, \qquad (3)$$

where $\beta(s)$ is the beta-function, $\langle\cdot\rangle_s$ is averaging along the ring, $Z_{x,y}$ is the transverse impedance. The transverse mode coupling instability (TMCI) happens when the tune shift matches the synchrotron tune. Above the threshold (indicated by blue and red dashed lines for closed and open IDs correspondingly), simulation results can deviate from the formula.

Then, we demonstrate the behaviour of the threshold for higher chromaticity in Fig. 7. Here, the black dotted and dashed lines correspond to the maximum bunch current for the standard and hybrid filling patterns respectively. We can disentangle horizontal and vertical instabilities by neglecting the vertical wake-fields in the horizontal-plane simulations and horizontal wake-fields in vertical-plane simulations. Passive measures to control the head-tail instabilities include operating at higher chromaticity and/or increasing the bunch length using the harmonic cavity. Unlike reported previously [2], the case of $\xi_x = \xi_y = 2$ (without other measures) is found to be insufficient enough for Diamond-II. As a result, we might need to increase vertical chromaticity to $\xi_y > 3$. This in turn may affect the dynamic aperture and lifetime, the impact of which remains to be determined.

Furthermore, a safety margin for impedance must be ensured. Fig. 8 demonstrates the results of simulations in the vertical plane where $\xi_x = \xi_y = 3$ is fixed while the total

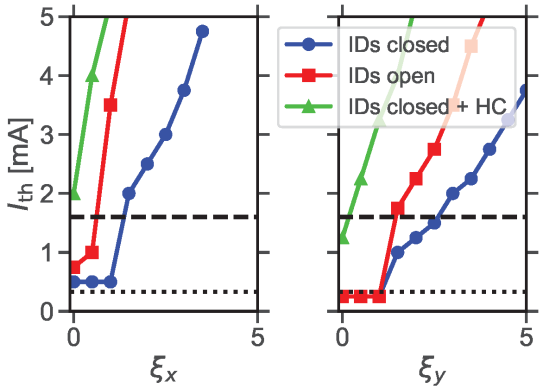

Figure 7: Instability threshold in the transverse plane with increasing horizontal (left) and vertical (right) chromaticity.

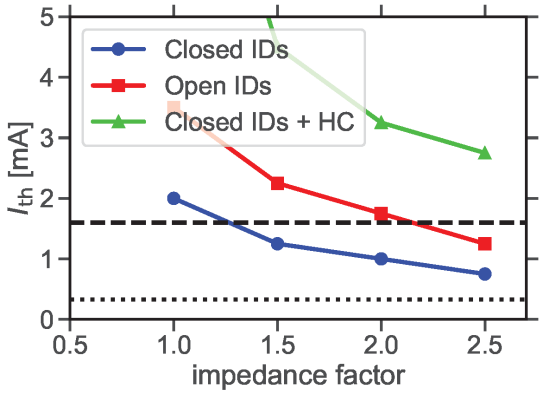

Figure 8: Transverse instability threshold vs the total impedance, chromaticities $\xi_x = \xi_y = 3$ are fixed.

impedance is scaled. In the case of closed IDs, the increase of the total impedance by a factor of 1.5 already limits the operation in hybrid mode (the threshold current is smaller than the hybrid bunch current). However, we can use the harmonic cavity. In this case, the hybrid-bunch current is safely below the threshold even if the total impedance is 2.5 stronger. In all cases, the nominal bunch current for the standard filling pattern remains below the instability threshold.

CONCLUSIONS

We have updated the impedance database and assessed wake-field effects in single-bunch dynamics. The results include current-dependent phase shift, bunch lengthening, momentum-spread increase, betatron tune shifts, and instability thresholds. In the case of open IDs, the machine can operate at the nominal value of chromaticity 2, whereas in the case of closed IDs, the harmonic cavity should be included for the hybrid filling pattern.

ISBN: 978-3-95450-231-8 ISSN: 2673-5490 doi: 10.18429/JACoW-IPAC2023-WEPL184

REFERENCES

[1] R. Fielder and T. Olsson, "Construction of an impedance model for Diamond-II", in *Proc. 12th Int. Particle Accel. Conf.*, Campinas, SP, Brazil, May 2021, pp. 455–458. doi:10.18429/JACOW-IPAC2021-MOPAB127

[2] R. Fielder, H.-C. Chao, and S. Wang, "Single bunch instability studies with a new impedance database for Diamond-II", in *Proc. 13th Int. Particle Accel. Conf.*, Bangkok, Thailand, May 2022, pp. 2257–2260. doi:10.18429/JACOW-IPAC2022-WEPOMS011

[3] A. Blednykh, G. Bassi, V. Smaluk, and R. Lindberg, "Impedance modeling and its application to the analysis of the collective effects", *Phys. Rev. Accel. Beams*, vol. 24, p. 104 801, 2021. doi:10.1103/PhysRevAccelBeams.24.104801

[4] D. Wang *et al.*, "Broadband impedance modeling and single bunch instabilities estimations of the advanced light source upgrade project", *Nucl. Instrum. Methods Phys. Res., Sect. A*, vol. 1031, p. 166 524, 2022. doi:https://doi.org/10.1016/j.nima.2022.166524

[5] Diamond-II Technical Design Report, Diamond Light Source, https://www.diamond.ac.uk/Home/News/LatestNews/2022/14-10-22.html, Accessed: 2023-04-25.

[6] CST Studio Suite, https://www.3ds.com/products-services/simulia/products/cst-studio-suite/, Accessed: 2023-04-19.

[7] ImpedanceWake2D, https://twiki.cern.ch/twiki/bin/view/ABPComputing/ImpedanceWake2D, Accessed: 2023-04-19.

[8] M. Borland, "Elegant: A flexible sdds-compliant code for accelerator simulation", 2000. doi:10.2172/761286